Pergamon

Int. J. Impact Engng, Vol. 19, No. 8, pp. 667–691, 1997

0734–743X/97 $17.00+0.00

PII:S0734-743X(96)00050-4

PLASTICITY, FRACTURE AND FRICTION IN STEADY-STATE PLATE CUTTING

BO CERUP SIMONSEN† and TOMASZ WIERZBICKI‡

†Department of Naval Architecture and Offshore Engineering, Technical University of Denmark, DK-2800 Lyngby, Denmark

‡Department of Ocean Engineering, Massachusetts Institute of Technology, Cambridge, MA 02139, U.S.A.

(*Received for publication* 16 *October* 1996)

Summary—A closed form solution to the problem of steady-state wedge cutting through a ductile metal plate is presented. The considered problem is an idealization of a ship bottom raking process, i.e. a continuous cutting damage of a ship bottom by a hard knife-like rock in a grounding event. A new kinematic model is proposed for the strain and displacement fields and it is demonstrated that the analysis is greatly simplified if the strain field is assumed to be dominated by plastic shear strains and moving hinge lines. Also, it is shown that the present shear model offers the basis for a convenient extension of the presented plate model to include more structural members as for example the stiffeners attached to a ship bottom plating. The fracture process is discussed and the model is formulated partly on the basis of the material fracture toughness. The effect of friction and the reaction force perpendicular to the direction of motion is derived theoretically in a consistent manner. The perpendicular reaction force is of paramount importance for predicting the structural damage of a ship hull because it governs the vertical ship motion and rock penetration which is strongly coupled with the horizontal resistance and thus with the damaged length. The derived expressions are discussed and compared with previously published experimental results and formulas. © 1997 Elsevier Science Ltd.

Keywords: plate cutting, ship grounding, ship bottom raking, crashworthiness.

NOTATION

$\dot{E}_c$	rate of energy dissipation in tip zone
$\dot{E}_m$	rate of energy dissipation for membrane deformation
$\dot{E}_b$	rate of energy dissipation for bending
F	total resistance force in the direction of motion
$F_{P,c}$	plastic and fracture resistance force
F_V	reaction force perpendicular to direction of motion
g	friction factor, $g=F/F_{P,c}$
G_c	material fracture toughness
k	vertical to horizontal force ratio, $k=F_V/F$
R	radius of plate curls at the side of the wedge
R_t	radius of plate curls at the front of the wedge, $R_t=R\cos\theta$
S	surface area of plate element
t	plate thickness
u	displacement in direction of ξ
u_o	gap opening at the wedge shoulder (Fig. 6)
v	displacement in direction of η
v_o	half gap opening at the wedge tip (Fig. 6)
α	angle between cutting edge normal to plate
χ	scaling parameter, (energy in farfield)/(energy in crack-tip zone)
ε_f	strain to fracture
η	coordinate perpendicular to material streamline
λ	geometric scaling factor
μ	coulomb coefficient of friction
σ_y	initial yield stress
σ_u	ultimate stress
σ_0	energy equivalent flow stress
θ	semi wedge angle, half of total angle between front sides
ξ	coordinate in the direction of material streamline
Others	defined where used

1. INTRODUCTION

One of the primary energy absorbing mechanisms in a grounding or collision event is the so-called plate cutting process. Most authors use the terms "cutting" or "tearing" although some of the observed failure modes are quite complex and have little resemblance to the original meaning of these words. The mechanics of the cutting process is complicated and involves plastic flow of the plate in the vicinity of the wedge tip (and, some would argue, fracture processes there) friction between wedge and plate, membrane deformation of the plate, and large scale bending of the plate "flaps" remote from the wedge tip into various scroll motifs and other folding patterns.

In this paper, the plate cutting phenomenon is described qualitatively, some of the most significant previous work is discussed and summarized, and new theories are derived for steady-state plate cutting by a wedge.

Depending on the deformation mode which develops, the plate cutting phenomena described in literature can be divided into three categories (see Fig. 1):

(1). *Stable or clean curling cut.* The plate is separated at the tip or in front of the wedge and rolls and folds to the same side during the entire process.
(2). *Braided cut.* The plate separates at the wedge tip as in the clean curling cut but the deformed flaps fold back-and-forth.
(3). *Concertina tearing.* The plate folds back-and-forth in front of the wedge while it is torn at remote boundaries.

The experimental and theoretical analyses of these three classes fall into two main categories:

(1). *Initiation or transient wedge penetration.* The wedge penetration is considered from the point of initial contact between wedge tip and plate edge to the point where the mean resistance force reaches a constant level. Normally the initiation phase can be assumed to terminate when the shoulders of the wedge enter the plate [13]. Since the maximum width of the penetrator in the plate increases with penetration, the reaction force is also an increasing function of the penetration. This process was initially considered as an idealization of a rigid ship bow penetrating into the deck-plating of another ship in a collision, but recently it has also been applied to groundings. Several authors (for example [18,5,] and [19]) have applied results or models for this process as an approximation to problems of "steady-state penetration" described below.
(2). *Steady-state penetration.* If the penetrator has a finite width, the plate reaction force will reach a constant mean level after a certain penetration and the process is then said to be in steady-state. This process is considered an idealization of a rock pinnacle or ice reef cutting through a ship bottom in a grounding or ice collision event.

For each of the three examples shown in Fig. 1, the deformation was large enough for the steady-state to be reached so the figure shows the deformation and the reaction in both the initiation and the steady-state phases.

The present paper is concerned with the clean curled cutting so whenever the term "cutting" is used in the following without further explanation it refers to this specific cutting mode.

2. PREVIOUS WORK

A thorough literature review was presented by Lu and Calladine [13], but since then the list of relevant publications has been expanded. A brief summary of literature pertinent to the field of plate cutting is given below.

The basic geometrical features of the cutting set-up used in the reported experimental work is shown in Fig. 2.

The definition of the inclination angle, α, varies; some perform experiments with an inclined plate and some incline the cutting edge as shown in Fig. 2.

Earlier experiments were performed with drop-hammer tests but to eliminate dynamic effects—which are difficult to interpret—most recent work is all based on quasi-static testing.

Several authors developed simple formulas giving the energy absorbtion, W, as a function of the penetration, l, in the plate. The reaction force, F, is then calculated from $W(l)$ as $F(l)=\mathrm{d}W/\mathrm{d}l$ with a

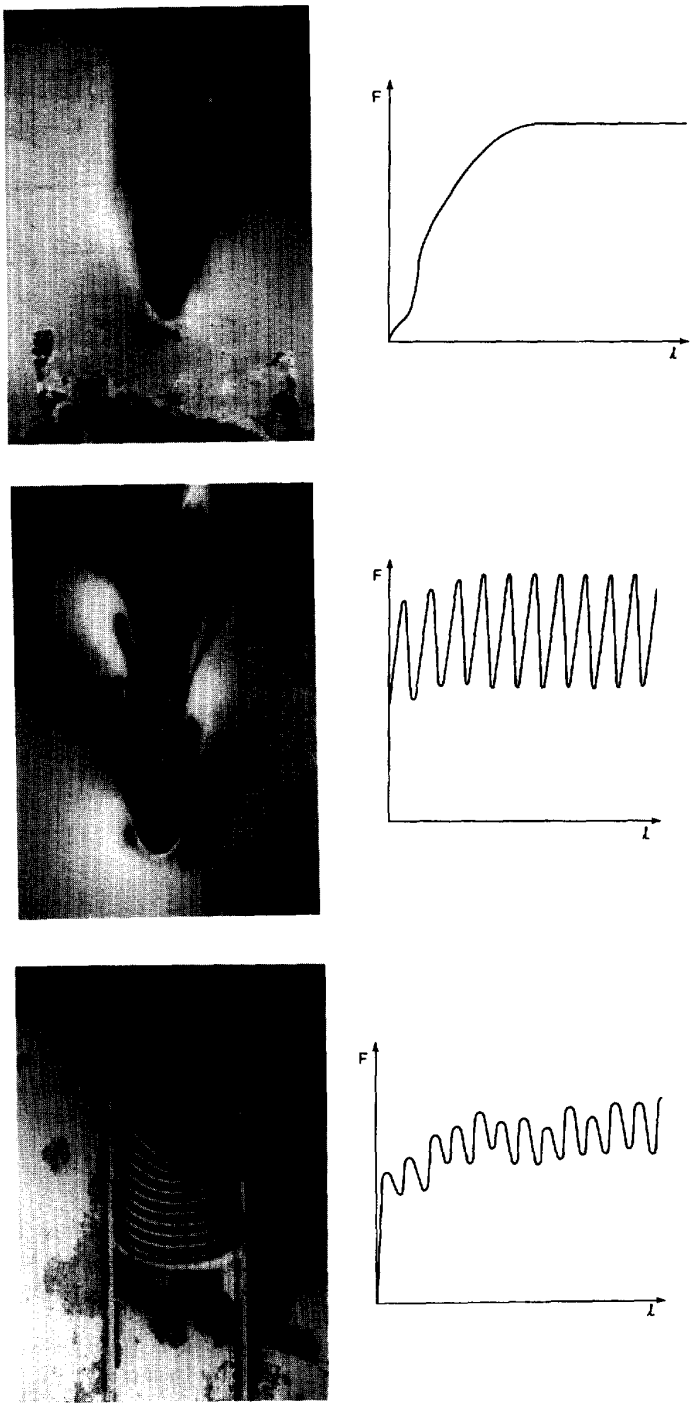

Fig. 1. Photographs of three cutting modes: clean curling cut, braided cut and concertina tearing with correspondence force–displacement (F,l)-digrams.

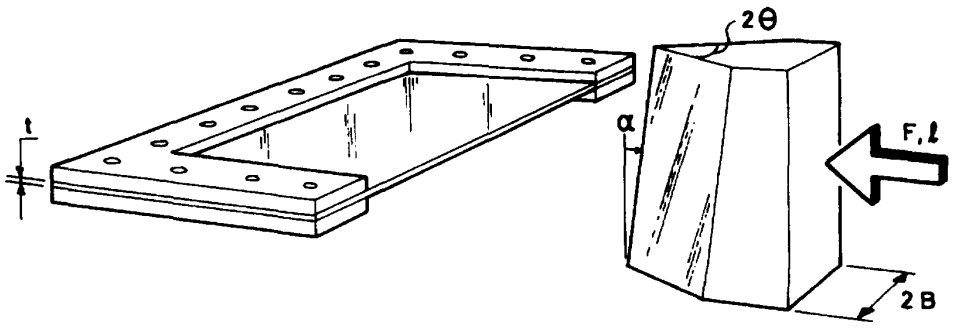

Fig. 2. Cutting set-up.

correction factor when needed due to the inconsistency of dimensions. In the next section the formulas are compared.

The notation used in the paper is given below.

F	reaction force from plate on wedge (N)
W	absorbed energy (Nm)
l	length of penetration into plate (mm)
t	plate thickness (mm)
δ_t	crack-tip opening displacement (mm)
$\bar{\delta}_t$	non dimensional crack-tip opening displacement, $\bar{\delta}_t = \delta_t/t$
2θ	wedge angle, i.e. angle between wedge faces
$2B$	shoulder width of wedge
b	spacing between longitudinal stiffeners
μ	coefficient of friction
α	angle between cutting edge normal to plate
σ_y	initial yield stress
σ_0	energy equivalent flow stress

Not all of the empirical formulas listed in the following are dimensionally consistent, i.e. they are not independent of the dimensions of the involved parameters. If not defined otherwise, F is in N, W is in Nm(=J), and l,t is in mm.

Akita, Ando, Fujito and Kitamura [2,3] conducted tests with penetration of a rigid wedge (θ=30°,40°) into a 3.2 mm steel plate to analyze the response of a ship side in a collision. They proposed a simple conceptual model in which the plate exerts a normal compressive stress of σ_y onto the plate over the nominal contact area. From static equilibrium the plate resistance force becomes

$$F = 2.0\,\sigma_y t\, l \tan\theta. \tag{1}$$

Since the portion of the plate in contact with the wedge is deformed due to tearing and denting, it was proposed to reduce the resistance force by 20%. However, the analysis does not take the actual deformation mode of rolling plate flaps consistently into account and as it is shown in Fig. 3; the proposed formula, Eqn (1), overpredicts the actual plate resistance.

Vaughan [29,30] used the experimental data of Akita and Kitamura [3] together with Minorsky's formula [17] to estimate the damage suffered by a ship bottom cut by a reef or ice. Vaughan assumed that the energy would be absorbed in two mechanisms, plastic deformation and creation of new surfaces by fracture, and thus came up with a two term empirical expression for the energy absorbtion:

$$W = 33.3\,l t + 0.093 l^2 t \tan\theta \tag{2}$$

$$F = 33300\,t + 0.19 l t \tan\theta \tag{3}$$

Vaughan subsequently performed 64 drop-hammer experiments with plates of mild steel [30], with t=0.752, 0.958, 1.181, 1.867 mm and θ=5°, 15°, 30°. Based on the same idea of two major energy

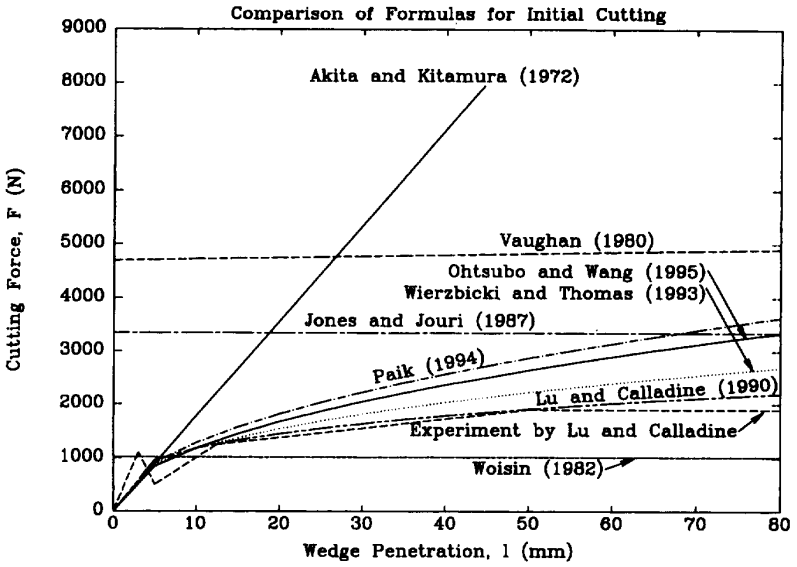

Fig. 3. Comparison of several formulas proposed in the literature with the result of one of Lu and Calladine's [13] experiments.

absorbing mechanisms, he obtained an expression for the energy absorption:

$$W = 5.5\, l t^{1.5} + 0.0044\, l^2 t^2 \tan\theta \tag{4}$$

$$F = 5500\, t^{1.5} + 8.8\, l t^2 \tan\theta. \tag{5}$$

All experiments were performed with the plate tilted an angle, $\alpha=10°$, because it was discovered that with this orientation, the cutting of the plates occurred by flaps rolling up on one side ("clean curling cut"), in contrast to the more complicated back-and-forth bending ("braided cut") which is characteristic when $\alpha=0°$.

The expression for the reaction force, Eqn (5), is seen to have a finite value at zero penetration so for small penetrations, these formulas do not correspond to actual reaction forces.

Woisin [34] analysed drop-hammer tests reported by GKSS in Germany. In a series of 13 tests, two equal plates (t=2–10 mm) cut into each other and Woisin proposed the following formula for the energy absorption:

$$W = 4.8\, l t^{1.7} \tag{6}$$

$$F = 4800\, t^{1.7}. \tag{7}$$

In a series of 19 tests, rigid wedges ($\alpha=0°$, $\theta=15°,35°,50°$) were forced into plates of mild steel with thicknesses between 2 and 4 mm. In seven of these tests the plate did not rupture although penetration amounted up to $l/t = 30$. The resistance of a plate of mild steel before fracture was found to be well approximated by the expression

$$F = 6000\, t^2 \tag{8}$$

when $12 \le l/t \le 30$ and 5 mm $\le l/t \le 10$ mm.

In the remaining cases where the plate ruptured the proposed expressions are:

$$W = 2.5\, l t^2 \left\{ 0.5 + 30\left(\frac{t}{l}\right) + \frac{\theta - 20°}{15°}\left(0.05 + 0.002\frac{l}{t}\right)\right\} \tag{9}$$

$$F = 2500 t^2 \left\{ 0.5 + \frac{\theta - 20°}{15°}\left(0.05 + 0.004\frac{l}{t}\right)\right\} \tag{10}$$

for $20° \le \theta \le 50°$ and $24 \le l/t \le 60$.

By considering the cutting response of plates of different thicknesses the complexity of scaling was noted.

Jones, Jouri, and Birch [9,11,12] performed drop-hammer tests on plates of mild steel. In the most recent work [11] 84 specimens were cut with $\alpha=0°$, $t=1.501$–5.95 mm, and $2\theta=30°,45°$ and $60°$. The energy absorbing mechanisms—cutting, bending, elasticity and friction—were identified and an attempt was made to partition the energy delivered between them. Bending and friction energy was found amounting to about 10% each, elasticity effects were neglectable, and the remaining, i.e. the energy absorbed in cutting was found to be given by the formulas:

$$W = 3.9\, l t^{1.44} \tag{11}$$

$$F = 3900\, t^{1.44} \tag{12}$$

for $t=1.501$ mm and $\sigma_0=255$ MPa and

$$W = 7.2\, l t^{1.305} \tag{13}$$

$$F = 7200\, t^{1.305}$$

for $t=3.25$, 4.955, 5.95 mm and $\sigma_0=398.5$ MPa.

It is seen that the reaction force is not a function of the penetration. This does not correspond to observations from quasi-static tests where the reaction force is a continuously increasing function of the penetration (see Fig. 1).

It is argued that material strain rate effects are insignificant for the test results. Scaling is discussed and it is illustrated that the geometrically similar scaling principles are not satisfied for the plate cutting problem.

Atkins [6] presents the scaling laws for bodies undergoing simultaneous plastic flow and crack propagation. Assuming rigid-plastic behaviour the energy scaling for prototype (p) and model (m) follows

$$\frac{W_p}{W_m} = \frac{\lambda^2(\lambda\chi + 1)}{\chi + 1} \tag{15}$$

where λ is the geometrical scale factor and χ is the ratio between the rate of energy dissipation in the far field deformation and the rate of energy in the crack-tip zone in one scale (provided the energy dissipation at the crack tip is proportional to the length scale squared and the energy dissipation in the far field is proportional to the length scale cubed).

It is argued that fracture is a governing parameter for the plate cutting process, [8]. By analysing the results of Jones, Jouri and Birch, [11,12], and Lu and Calladine [13], Atkins made an attempt to separate the energy dissipating mechanisms and find the variance of χ. Several difficulties were encountered though, and it seems that more experimental data would be needed before an approach of scaling is applicable to practical problems. It should be noted that in the work outlined below (for example Lu and Calladine [13]) all energy is assumed to be dissipated in plastic flow so the scaling of energy, W_p/W_m, follows λ^3 corresponding to $\chi=\infty$.

Lu and Calladine [13] performed quasi-static cutting tests with 35 case hardened plates of mild steel ($t=0.72$–2.0 mm, $\alpha=0°,10°,20°$ and $2\theta=20°,40°$) and by using Buckingham's dimensional analysis they found the formula:

$$\begin{aligned} W &= C_{1.3}\sigma_y l^{1.3} t^{1.7} \quad \text{for } 5 < l/t < 150 \\ F &= 1.3 C_{1.3}\sigma_y l^{0.3} t^{1.7} \quad \text{for } 5 < l/t < 150 \end{aligned} \tag{16}$$

where $C_{1.3}$ is a purely empirical constant which depends on the cutting conditions such as wedge and tilt angles. Unlike Eqns (2–14), the formulas by Lu and Calladine are seen to be dimensionally consistent.

As it will be discussed in more detail later, Lu and Calladine made valuable contributions to the field by discussing the effect of friction, fracture and dynamics. Also, the first attempt to investigate the effect of a finite shoulder width and thus the phase of steady-state cutting is presented in Ref. [13].

Wierzbicki and Thomas [33] developed an analytical model for prediction of the cutting force and derived an expression, identical in form and characteristics to the results presented by Lu and Calladine:

$$F = 3.28\, \sigma_0 \mu^{0.4} l^{0.4} t^{1.6} \delta_t^{-0.2} \tag{17}$$

for a coefficient of friction, $0.1 < \mu < 0.4$ and a wedge angle, $10° < \theta < 30°$. It is the first publication where a coefficient of friction, μ, and a fracture parameter, $\bar{\delta}_t$, enters the expression explicitly.

Paik [19,20] investigated the cutting response of stiffened steel plates. In Ref. [19], the analysis is based on dimensional analysis, 50 cutting experiments (t=3.4–7.8 mm, 2θ=15°,45°,60°), and the hypothesis that longitudinal stiffeners can be included by using an area equivalent plate thickness, t_{eq}. By applying a least-square best fit to the experimental data, Paik expressed the energy absorption and the cutting force as

$$W = C_{1.5} C_f \sigma_0 t_{eq}^{1.5} l^{1.5} \tag{18}$$

$$F = 1.5 C_{1.5} C_f \sigma_0 t_{eq}^{1.5} l^{0.5} \tag{19}$$

with the coefficient, $C_{1.5}$, being a function of wedge angle alone:

$$C_{1.5} = 1.112 - 1.156\theta + 3.760\theta^2 \tag{20}$$

and the dynamic correction factor, C_f, expressed as a function of the initial impact velocity, V, as

$$C_f = 1.0 - 0.042V + 0.001V^2. \tag{21}$$

In accordance with Lu and Calladine [13], Paik considered inertia effects to be negligible whereas strain rate effects tend to raise the load level and dynamic effects on friction tend to lower the load. However, it is interesting to note that C_f is found to be a decreasing function of the impact velocity, for example C_f=1 at V=0 m/s and C_f=0.67 at V=8 m/s. It should be noted that the correction factor C_f is found from the drop-hammer results of Jones and Jouri [11]. In drop-hammer tests the velocity decreases from V to zero but this change in velocity has not been taken into account in the derivation of C_f so Eqn (21) cannot necessarily be used in Eqn (19) for an instantaneous velocity.

In Ref. [20], Paik and Lee discuss the effect of transverse stiffeners and it is proposed that these should be included in the analysis in a discrete manner (as opposed to the continuous 'smearing' technique proposed for longitudinal members).

Wierzbicki [31] developed a closed form solution for the reaction force when a concertina tearing deformation mode develops (see Fig. 1). By assuming a deformation mode and applying the principle of virtual work, the mean resistance force was found to be

$$F = 2\sqrt{3}\sigma_0 t^2 \left[\frac{2}{\sqrt{3}} \left(\frac{b}{t} \right)^{1/3} + \frac{\delta_t}{t} \right]. \tag{22}$$

Experimental results with plates of mild steel (t=0.74–1.14 mm) are presented for validation of the model.

Astrup [5] conducted experiments (2θ=60°, α=10°, $2B$=250 mm, t=15,20 mm) to investigate the cutting of thick plates with a wedge of finite width. The observed failure modes were quite complex, in that both stable plate cutting and concertina tearing modes were seen. It is noted in Ref. [5] that the measured reaction force was generally 60–75% higher than that predicted by the formula of Lu and Calladine. It is argued that this difference is due to strain rate effects and frictional effects. Another reason is that the test wedge had a finite shoulder width whereas the formula of Lu and Calladine is based on the initial penetration. This means that after the wedge shoulders have entered the plate a cutting mode different to that observed in Lu and Calladine's experiments will develop. Large scours were observed on the cut specimens and it is argued that a coefficient of friction equal to 0.5–0.55 seems reasonable. By comparing the energy absorbtion in the *initial* deformation with the drop-hammer tests of Jones *et al.* [11], it is found that there are no significant size effects in the cutting phenomenon.

Zheng and Wierzbicki [36] developed a closed form solution for the reaction force after steady-state is reached. It is assumed that the cutting process consists of three different energy absorbing mechanisms:

1. ductile fracture in a small zone in front of the wedge;
2. bending of the plate in moving hinge lines; and
3. membrane deformation.

A suitable model was postulated for the kinematics with one free parameter, the so-called plate rolling radius R. The rate of energy dissipation in each of the three mechanisms listed above is expressed as a

function of this rolling radius. In compliance with the idea of a least upper bound, the total resistance is found by minimizing the total resistance force with respect to the rolling radius.

The resistance force is given by

$$F = \frac{\sigma_0 t^2}{4}\left[2\frac{B+R}{R} + 1.27\frac{R}{t}\cos\theta + 1.28\theta^2\frac{\cos(\theta/2)}{\cos\theta}\frac{(R+B)^2}{Rt}\right](1+\mu\cos\theta) \tag{23}$$

with the rolling radius,

$$R = B\sqrt{\frac{2(t/B) + 1.28\theta^2\cos(\theta/2)/\cos\theta}{1.27\cos\theta + 1.28\theta^2\cos(\theta/2)/\cos\theta}}. \tag{24}$$

Ohtsubo and Wang [18] present an analysis method somewhat similar to that of Wierzbicki and Thomas [33]. A kinematic model is proposed and the energy dissipation of the plastic flow in the tip zone and in rolling hinge lines is calculated. The proposed expression for the cutting force is

$$F = 1.51\sigma_0 t^{1.5} l^{0.5}\sin^{0.5}(\theta)\left(1 + \frac{\mu}{\tan\theta}\right). \tag{25}$$

3. COMPARISON OF FORMULAS FOR INITIATION CUTTING

As a general comparison of the proposed formulas is difficult this section compares the formulas for two specific setups; cutting of a thin (0.9 mm) plate of mild steel and cutting of a high-strength steel plate with a thickness (15 mm) relevant for ship building. It should be noted that a few of the formulas are shown outside the proposed range of validity.

Fig. 3 shows a comparison of the proposed formulas with the results of one of the experiments reported in Ref. [13]. The input data for the calculations are given in Table 1.

It is seen that overall there is significant difference between the formulas. However, the latest formulas proposed by Lu and Callidine [13], Wierzbicki and Thomas [33], Paik [19], and Ohtsubo and Wang [18] show a similar trend which corresponds quite well with the experimental result.

Fig. 4 shows a comparison of the proposed formulas with the results of one of the experiments reported in Ref. [5]. The input data for the calculations are given in Table 2.

As in Figs 3 and 4 shows a considerable scatter between theoretical predictions. It is seen that up to the point (l=216 mm) where the wedge shoulders enter the plate there is a fair correspondence between most of the formulas and the experimental curve.

Table 1. Main data for comparison example with experiment of Lu and Calladine

Plate thickness, t	0.9 mm
Wedge angle, 2θ	40°
Flow stress, $\sigma_0=\sigma_y$	272 MPa
Coefficient of friction, μ	0.3
Nondimensional crack opening displacement, $\bar{\delta}_t$	1
Length of penetration, l	0–80 mm

Table 2. Main data for comparison example with experiment Astrup [5]

Plate thickness, t	15.0 mm
Wedge angle, 2θ	60°
Yield stress σ_y	417 MPa
Flow stress, $\sigma_0=\sigma_u$	544 MPa
Coefficient of friction, μ	0.3
Nondimensional crack opening displacement, $\bar{\delta}_t$	1
Length of penetration, l	0–432 mm

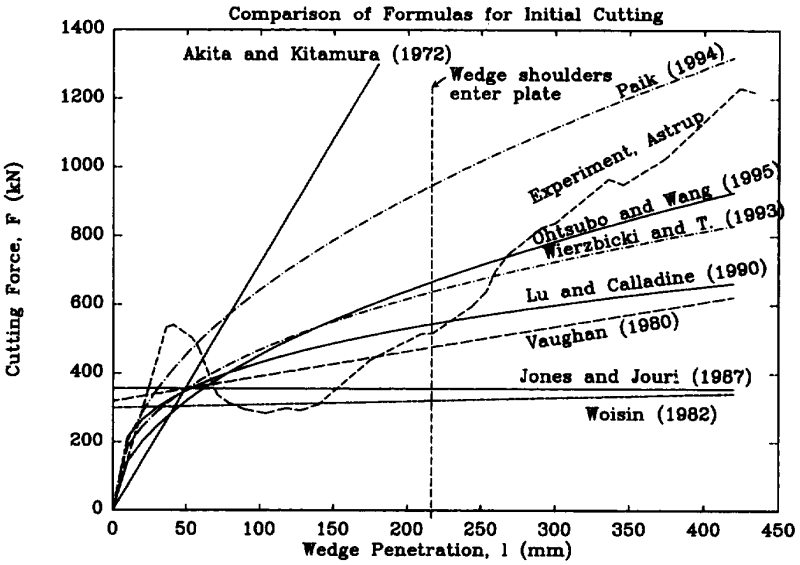

Fig. 4. Comparison of several formulas proposed in the literature with the result of one of Astrup's experiments [5] for a 15 mm plate. The wedge shoulders enter the plate at l=216 mm.

4. PREDICTION OF STEADY-STATE CUTTING FORCE

Lu and Calladine [13], Paik and Lee [20], Astrup [5], Yahiaoui *et al.* [35], and Zheng and Wierzbicki [36] performed tests with wedges of finite width; however, the only formula in which the wedge width enters explicitly is due to Zheng and Wierzbicki [36]. The experimental results of Lu and Calladine [13], Yahiaoui *et al.* [35] and Astrup [5], are summarized in Table 3. In all of the reported tests the wedge angle was inclined an angle α=10° in order to obtain the clean curling cutting mode shown in Fig. 1.

Lu and Calladine [13] observed that the main features of the physical behaviour and of the resulting load-deformation curve are of the same kind as initiation cutting until the upper edge of the plate reaches the shoulder of the wedge, whereupon the resisting force remains practically constant as the wedge penetrates further. On the other hand Thomas [27] found that the initiation phase goes beyond the point where the shoulders enter the plate—it is rather twice as long, as suggested by Lu and Calladine. The experimental curve of Astrup shown in Fig. 4 does not show a distinct penetration at which steady-state is reached because the deformation initiates a mode of braided cutting (see Fig. 1). Based on the observations of Thomas [27] and Lu and Calladine [13], it seems realistic to use the proposed formulas for initiation cutting up to a certain point of penetration, l, and assume that the load level is retained from this point of penetration throughout the rest of the deformation. This penetration, l, is then

$$l = \kappa_{\text{ini}} \frac{2B}{\tan\theta} \tag{26}$$

with $\kappa_{\text{ini}} = 1 - 2$. Table 4 presents results of this approach, i.e. the penetration, l, of Eqn (26) is used in the formulas for initiation cutting, Eqns (16,17,19,25). Corresponding to the findings of Lu and Calladine and Thomas the value of κ_{ini} is taken as, respectively, 1 and 2 in Table 4. Clearly, the approach

Table 3. Experimental results for steady-state cutting. In all experiments the wedge was inclined an angle, α=10°

Experiments by	σ_0 (MPa)	θ (°)	$2B$ (mm)	t (mm)	F (kN)
1. Lu and Calladine [13]	272	10	10	1.6	6.0
2. Yahiaouli *et al.* [35]	270	45	19	0.75	2.5
3. Astrup [5]	526	30	250	20	2250

Table 4. Theoretical prediction of steady-state cutting for the experimental results of Table 3. The following abbreviations are used for the formulas: L/C: Lu and Calladine [13], W/T: Wierzbicki and Thomas [33], O/W: Ohtsubo and Wang [18], Z/W: Zheng and Wierzbicki [36]

Experiments by	Theoretical prediction:$\kappa_{ini}=1$					Theoretical prediction:$\kappa_{ini}=2$			
	L/C Eqn (16)(kN)	W/T Eqn (17) (kN)	Paik Eqn (19) (kN)	O/W Eqn (19) (kN)	Z/W Eqn (23) (kN)	L/C Eqn (16) (kN)	W/T Eqn (17) (kN)	Paik Eqn (19) (kN)	O/W Eqn (25) (kN)
1. Lu and Calladine [13]	5.81	5.88	6.37	7.05	3.81	7.15	7.76	9.01	9.97
2. Yahiaoui *et al.* [35]	1.14	1.12	2.89	1.26	3.28	1.41	1.48	4.08	1.78
3. Astrup [5]	1514	1459	2258	1588	1580	1864	1925	31.93	2246

is approximative because the deformation pattern shifts from a mode of cutting and curling in the initiation mode to a mode of cutting, curling and membrane deformation in the steady-state phase. The particular deformation mode of the steady-state phase was considered by Zheng and Wierzbicki [36] who derived Eqn (23).

The input values to the formulas used in Table 4 (B, t etc.) are taken corresponding to the experimental results presented in Table 3. The coefficient of friction is assumed to be $\mu=0.3$.

As in Figs 3 and 4, the difference between various theoretical predictions is seen to be quite remarkable. It is interesting to note that the formula of Paik Eqn (19) corresponds well with all of the observed results when $\kappa_{ini}=1$ is used. It should be noted that if the coefficient of friction is increased to $\mu=0.55$ as proposed by Astrup [5], the theoretical prediction for Astrup's results of Ohtsubo/Wang ($\kappa_{ini}=1$) and Zheng/Wierzbicki rise from 1588 kN, 1580–2041 kN and 2030 kN, respectively. These results are seen to correspond quite well to the experimental value of 2250 kN.

5. PROBLEM STATEMENT AND BASIC IDEA OF MODEL

The remainder of the present paper is concerned with derivation and verification of a theoretical model for analysis of steady-state cutting of a metal plate by a prismatic wedge.

The ultimate goal of these studies is to analyse an assembled ship bottom structure which is significantly more complex than just a bare plate. The approach taken here is to postulate the displacement and strain fields and then, by use of the principle of virtual work, find the resisting force of the plate. The advantage of this type of approach over a purely experimental one is that once the major deformation and energy dissipating mechanisms are identified, it is possible to consistently add stiffeners to the plate and find the energy dissipation and resisting force of the total assembled structure, (see Ref. [23]). To derive general expressions for the resistance of such a hull bottom assembly from experimental data alone seems to be an overwhelming task. The idea of smearing longitudinal stiffeners presented by Paik [19] is promising, but for use in design of complex structures it would seem unable to capture all the effects of structural details.

The basic idea of the present approach is illustrated below. A prismatic wedge cuts through a ductile plate which is assumed to deform as shown in Fig. 5. Since the process is considered to be in steady-state, this picture of the deformation does not change in time. Dynamic effects are not included in the present analysis, although it is recognized (see e.g. Jones [10]) that these could be significant for full scale grounding problems where the impact speed may be up to 45 knots (23 m/s).

There are three energy dissipating mechanisms in the considered deformation mode:

- moving hinge lines;
- membrane deformation of the plate; and
- material separation in the crack-tip zone.

In reality, there is no clear distinction between these mechanisms but it has been shown in several areas of sheet metal deformation and fracture that such a separation of energy absorbing mechanisms often adequately represent the observed behaviour leading to great simplifications of the theoretical analysis, (see e.g. Atkins [6], Alexander [4], and Wierzbicki and Abramowicz [32]).

It is worth to note that the material flows *through* the deformation zone shown in Figs 5 and 6 in contrast to many structural problems where the volume of deformation is stationary within the structure.

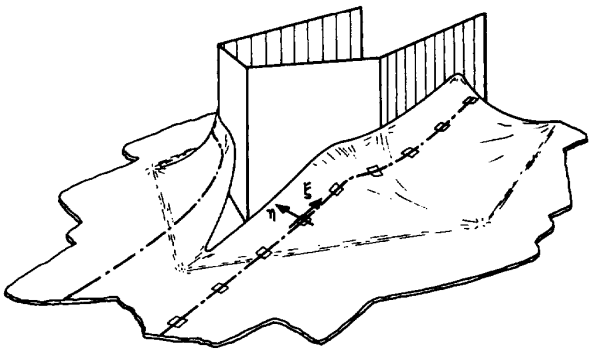

Fig. 5. Assumed mode of the deformation.

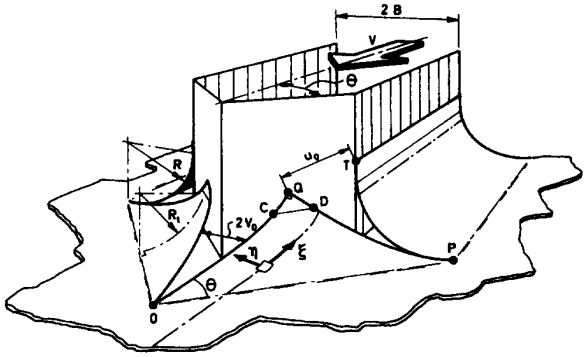

Fig. 6. Necessary straining illustrated by gap width.

The present deformation pattern resembles one of fluid flow around a blunt body. Similar to most fluid flow solutions, a Eulerian description of motion is used. As illustrated in Fig. 5 the material flow is described in a (ξ, η) coordinate system where ξ follows the streamlines and η is in the perpendicular direction. As a material element moves along a streamline it experiences bending as it passes the OP-line followed by a continuous increasing shear deformation as it moves towards the wedge shoulder. If the material element is close to the centerline, it experiences an additional tensile deformation in the perpendicular $(\eta-)$ direction as it passes the zone of plate separation in front of the wedge.

5.1. Moving hinge lines

The moving hinge line OP in Fig. 5 changes the curvature of the undisturbed plate from $0–1/R_t$ and the hinge line CD reverts the curvature back to zero so that there is a straight plate flap conforming to the wedge sides. The rolling radius, R_t is kept as a variable in the formulation and taken as the value which gives the lowest rate of energy dissipation. In the wake of the wedge, the rolling radius is $R = R_t/\cos\theta$. The assumed mode of deformation with plane flaps conforming to the wedge corresponds well to the experimental observations of Astrup [5], Yahiaoui [35], Rodd and MacCampbell [22], and Lu and Calladine [13].

5.2. Membrane deformation

Figure 6 shows the geometry that is seen if the plate was cut at the center line and along the edges PT, PQ and folded without membrane deformation of the plate (this could be done with a piece of paper and a pair of scissors). Then, the gaps between the plate edges PT and PQ are indicative of the amount of membrane straining necessary for material continuity during the cutting process. In the large scale tests

of Astrup [5], a few lateral cracks were also observed (along line PT in Fig. 6) but for thin plates this is not seen.

The necessary straining can be accommodated by an infinite number of possible strain fields. The actual strain rate field is the one that minimizes the instantaneous rate of energy dissipation of material flow, fracture and friction. Little is published about the strain field in steady-state cutting, but useful information can be obtained from inspection of cut specimens. The cut plate will transmit direct tensile (or compressive) stresses in the ξ direction, and likewise tensile strains will develop. This can be deduced from Fig. 1 for the curled cut where the deformed plate is seen to be buckled. During the cutting process the longitudinal plate fibres are stretched in the deforming zone at the wedge front, and instead of recompressing back to the original length leaving straight flaps in the wake, the plate buckles. As mentioned, however, the plating of a ship structure has stiffeners attached to it and the presence of longitudinal stiffeners which are often quite substantial tend to prevent the development of tensile deformation in the longitudinal direction of the hull structure when the deformation is large enough for the longitudinal to be involved.

The hull plating will rather deform in a mode where longitudinal fibres are sheared with respect to each other. Such a deformation mode predominantly shear of in the (ξ, η) coordinate system (see Fig. 5) was reported by Turgeon [28] for small scale tests without fracture and by Rodd and MacCampbell [22] for large scale grounding tests with a double bottom being deformed by a conical rock. Fig. 7 shows the failure mode of the test reported by Rodd and MacCampbell [22]. Significant shear bands are observed in the bottom plating.

Also, in the large scale cutting tests of Astrup [5], the deformed plate flaps were seen to be nearly plane, indicating shear rather than tensile deformation. Based on these observations, the present formulation for the membrane deformation rests on the assumption that the in-plane strains in the far

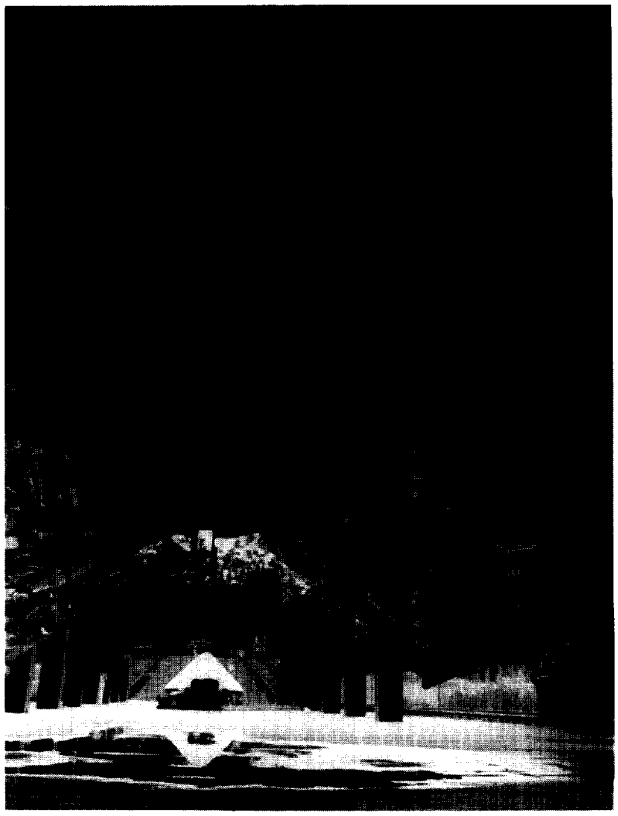

Fig. 7. Failure mode of ship bottom observed in NSWC Test No. 1 [22], (frog's eye view).

field are all shear strains. It is recognized that this is not always the case but as it will be argued later this assumption greatly simplifies the analysis. Since longitudinal fibres are not stretched, the present model also provides a realistic basic deformation pattern model for the case of a longitudinally stiffened plate.

5.3. Near tip plate separation

Although the process of the near tip crack zone has been considered explicitly by several authors, no one has yet applied a theory to the problem of plate cutting which covers in detail and generality the material splitting process. Lu and Calladine [15] argue that the cutting process can be described at a sufficient level of accuracy with the flow stress as the only material parameter. A discussion on this topic is given by Atkins and Lu [8] and Calladine [14]. Stronge *et al.* [25,26] performed an experimental and theoretical study on the problem of tube splitting and concluded that the relative contribution of the tearing energy to the total energy dissipation is small. This supports the presented analyses in Section 2 where fracture parameters are not included. Several authors leave material fracture parameters out of the analysis based on the observation that the crack tip stays right at the wedge tip so that the separation process is one of plastic flow rather than fracture. For highly ductile specimens as those thin plates of mild steel used in several of the reported model tests are being cut by a sharp wedge is true and not too surprising that the plate separates at the cutting edge. However, for less ductile specimens—for example thick hull plating [5], or other types of material [13]—or blunt nosed wedges [22,16], the crack was observed to run ahead of the wedge and a general theory should therefore cover this situation and thus consider the fracture toughness of the material.

In the large scale double bottom grounding tests reported in Ref. [22], an unstable crack was seen to unzip a part of the structure in front of the wedge. A stable crack in the outer bottom propagated with the penetration of the rock, but at a certain point of penetration the crack suddenly propagated through a transverse bulk head far into the inner hull plating. To capture this complex type of behaviour would require very detailed elasto-plastic calculations. Theoretically, the finite element method would be applicable but for practical use in design it is too labour intensitive so the present approach is based on a less accurate rigid-plastic analysis.

The question of whether fracture should be included or not is handled in our mathematical model by choosing between purely plastic flow or fracture depending on which of the two alternative modes gives the lowest energy dissipation. This corresponds to normal fracture criteria for ductile materials (see for example Atkins [7]).

6. BASIC EQUATIONS FOR PLASTICITY, FRACTURE AND FRICTION

When external loads are applied to a deformable structure, the power of these loads must be equal to the incremental energy stored elastically or dissipated in the structure. Assuming a rigid-plastic structure, no elastic energy can be stored and the power of the external loads thus equals the rate of energy dissipated by plastic deformations, fracture and frictional effects on the structure surface. This can be expressed as

$$F \cdot V = \dot{E}_{\mathrm{p}} + \dot{E}_{\mathrm{c}} + \dot{E}_f = F_{P,c} \cdot V + \int_S p\mu V_{\mathrm{rel}} \mathrm{d}S, \tag{27}$$

where:

F	the resisting force of the structure in the direction of V
V	the relative velocity between ship and rock
$\dot{E}_{\mathrm{p}}$	the rate of plastic energy dissipation
$\dot{E}_{\mathrm{c}}$	the rate of energy dissipation in the crack-tip zone
$\dot{E}_f$	the rate of energy dissipated by frictional forces on the surface of the structure
$F_{P,c}$	the so-called plastic resistance which here includes both plasticity and fracture
μ	the Coulomb coefficient of friction
p	the normal pressure on the rock from the plate element, dS
S	denotes the contact area between rock and plate
V_{rel}	the relative velocity between rock and plate element, dS

In the present model, the internal energy dissipation and frictional effects are considered separately without coupling. Kinematically admissible displacement fields are constructed according to Fig. 6 and from the assumed deformation fields, the corresponding rates of energies, $\dot{E}_p$, $\dot{E}_c$ and $\dot{E}_f$ are calculated. The assumed kinematics of the deformation has one free parameter, the plate rolling radius R, and it is postulated that the actual deformation mode is the one that minimizes the total rate of energy dissipation.

Supporting our approach, Atkins [6,7] has shown that the rigid-plastic approximations to tearing problems of ten adequately represent observed behaviour when fracture is accompanied by, or preceded by, extensive plastic flow. Examples (other than plate cutting) which include both fracture and far field deformation are tensile tearing of a deep double edge notched (DEN) specimens and trouser tearing. The basic idea of the methods for finding the specific work of fracture, G_c, is to perform experiments to determine all parameters, but $\dot{E}_c$ in Eqn (27). Then, from $\dot{E}_c$ and the kinematics of the specific problem, G_c can be determined. As mentioned, the distinction between a crack-tip zone and the far field presented by Atkins is also applied in the present analysis.

6.1. Plastic energy dissipation in far field

With rigid-plastic material obeying von Mises yield criterion the plane stress yield condition can be written as

$$F = \sigma_{xx}^2 + \sigma_{xx}\sigma_{yy} + \sigma_{yy}^2 + 3\sigma_{xy}^2 - \sigma_0^2 = 0 \tag{28}$$

where σ_0 is the uniaxial yield stress. For real construction materials σ_0 is a function of strain history and strain rate. Here, σ_0 is considered constant and equal to an average flow stress for the considered process. Thus, the flow stress is higher than the initial yield stress but lower than the ultimate stress, σ_u. Following Abramowicz and Wierzbicki [1], an estimate of the energy equivalent flow stress is $\sigma_0 = 0.92 \cdot \sigma_u$.

For a deforming plate of area S, the rate of internal energy dissipation can be expressed as

$$\dot{E}_p = \dot{E}_m + \dot{E}_b = \int_s N_{\alpha\beta}\dot{\varepsilon}\alpha\beta \mathrm{d}S + \int_S M_{\alpha\beta}\dot{\kappa}\alpha\beta \mathrm{d}S \tag{29}$$

where $N_{\alpha\beta}$, $M_{\alpha\beta}$ are components of the membrane force and bending moment tensors, and $\dot{\varepsilon}\alpha\beta$, $\dot{\kappa}\alpha\beta$ are the corresponding generalized strain and curvature rates calculated in the deformed configuration. The two terms in the above equation represent the rate of membrane and bending energy dissipation, $\dot{E}_m$ and $\dot{E}_b$, respectively. In general $N_{\alpha\beta}$ and $M_{\alpha\beta}$ in Eqn (29) are related by the yield condition, Eqn (28). However, this interaction between moments and membrane forces is very cumbersome to handle analytically and it is neglected in the present analysis.

It is assumed that the deformation zone consists of a series of discrete moving hinge lines and a number of deforming plate elements. Taking the rock to be stationary, the hull deformation can be thought of as a steady-state flow of hull material past the rock. Since the material moves *through* a deformation zone, it is convenient to introduce a spatial-Eulerian coordinate system (ξ,η), where ξ is directed along the material stream lines and η is perpendicular to them (see Figs 5 and 6).

The material derivative of a given quantity [ ] is, in general, composed of two parts;

$$\frac{D[\,]}{Dt} = \frac{\partial[\,]}{\partial t} + \nabla[\,].\mathbf{V}_\alpha \tag{30}$$

where the components of the gradient vector, ∇ and velocity vector, $\mathbf{V}_\alpha$, are:

$$\nabla = \begin{bmatrix} \partial/\partial\xi \\ \partial/\partial\eta \end{bmatrix} \quad \mathbf{V}_\alpha = \left[\frac{\partial\xi}{\partial t}, \frac{\partial\eta}{\partial t}\right]. \tag{31}$$

For a steady-state process, the time change of any quantity, [ ], at a given location is zero. Therefore, the first term in Eqn (30) vanishes. Furthermore, since material points follow the stream lines with a velocity of V, $\partial\eta/\partial t = 0$ and $\partial\xi/\partial t = V$. Therefore, for steady-state flow Eqn (30) reduces to

$$\frac{D[\,]}{Dt} = V\frac{\partial[\,]}{\partial\xi}. \tag{32}$$

The rate of membrane energy dissipation in Eqn (29) for a plate strip of width $d\eta$ can be expressed as

$$d\dot{E}_m = t \int_{\xi_a}^{\xi_b} \sigma_{\alpha\beta}\dot{\varepsilon}_{\alpha\beta} d\xi d\eta \tag{33}$$

where (ξ_a, ξ_b) are boundaries of the local plastically deforming zone. By using the yield condition, Eqn (33) can be written as

$$d\dot{E}_m = \frac{2}{\sqrt{3}}\sigma_0 t \int_{\xi_a}^{\xi_b} \sqrt{\dot{\varepsilon}_{\xi\xi}^2 + \dot{\varepsilon}_{\eta\eta}^2 + \dot{\varepsilon}_{\xi\xi}\dot{\varepsilon}_{\eta\eta} + \dot{\varepsilon}_{\xi\eta}^2}\, d\xi d\eta. \tag{34}$$

For a steady-state process Eqn (32) can be used to transform the timely strain derivatives of Eqn (34) into space derivatives. Then, by assuming proportional strain paths and performing the integration over the length of the deformation zone from ξ_a to ξ_b, the expression for the rate of membrane energy dissipation becomes

$$d\dot{E}_m = \sigma_0 V t[\varepsilon_{eq}] d\eta \tag{35}$$

where $[\varepsilon_{eq}]$ is the change in equivalent strain of a material element from entering to leaving the deformation zone. The equivalent strain is given by

$$\varepsilon_{eq} = \frac{2}{\sqrt{3}}\sqrt{\varepsilon_{\xi\xi}^2 + \varepsilon_{\eta\eta}^2 + \varepsilon_{\xi\xi}\varepsilon_{\eta\eta} + \varepsilon_{\xi\eta}^2}. \tag{36}$$

Using Eqn (32) it can be shown [24], that the rate of bending energy dissipation, $d\dot{E}_b$, for a plate strip of width $d\eta$ is

$$d\dot{E}_b = V_n M_0[\kappa_{nn}] dL = V M_0[\kappa_{nn}] d\eta \tag{37}$$

where dL is the length of the hinge line, $[\kappa_{nn}]$ is the jump in curvature over a hinge line, V_n the normal velocity of the hinge line, and M_0 is the plane strain fully plastic bending moment per unit length:

$$M_0 = \frac{2}{\sqrt{3}}\frac{\sigma_0 t^2}{4}. \tag{38}$$

Expression (37) should be integrated over all hinge lines appearing in the given problem.

6.2. *Energy dissipation in crack-tip zone*

As mentioned in Section 5 several different views on how to treat the tip zone process theoretically have been presented. One approach is to use the ductile fracture toughness, G_c, giving a rate of energy dissipation in the tip zone of

$$\dot{E}_c = G_c \dot{A} = G_c t V \tag{39}$$

where $\dot{A} = tV$ is the rate by which new area is generated.

One disadvantage with use of Eqn (39) G_c is highly dependent on the actual strain history up to the point of fracture. For mild steel, Atkins [17] reports values of G_c ranging from 200–1000 kJ/m^2 depending on the fracture mode, so carefully planned experiments have to be carried out to determine the actual values of G_c.

For very ductile materials or narrow sharp wedges the plate does not separate in a true fracture mode but the material is rather forced to flow around the wedge making the use of a fracture toughness parameter questionable. The rate of energy dissipation for this alternative mode of purely plastic flow is an integral over the volume of the tip zone:

$$\dot{E}_c = \int_s \sigma_0 \dot{\varepsilon}_{eq} t \, dS_{\text{tip zone}}. \tag{40}$$

The choice of deformation mode in the present formulation is based on the standard fracture mechanics approach of choosing the deformation mode Eqn (39) or Eqn (40) that gives the lowest rate of energy dissipation.

7. ENERGY DISSIPATION IN PLASTICITY AND FRACTURE

The basics for the development of the expressions for the rate of energy dissipation in the tip zone and in the far field has been described in Sections 5 and 6. The final expressions are derived below. The deformation in the far field is divided into membrane deformation and bending.

7.1. Tip zone

The energy dissipation rate for this process is given by Eqns (39) and (40). In order to evaluate the integral of Eqn (40) we assume that the strain field is dominated by tensile strains in the lateral (η) direction. This is not fully consistent with the assumption that the PT–PQ gap in Fig. 6 is accommodated by shear strains alone, but estimates indicate that the effect of shear in the tip zone is small. Indeed, due to symmetry, the shear must be zero at the center line. Following Eqn (40) it is sufficient to consider the total equivalent strain of the material in the wake of the cutting edge. With $\varepsilon_{\xi\xi}=\varepsilon_{\xi\eta}=0$, the final expression is found as an integral over the width of the plastic zone in the wake of the cutting edge:

$$\dot{E}_c = 2\sigma_0 Vt \int [\varepsilon_{eq}] d\eta \tag{41}$$

$$= 2\sigma_0 Vt \int_{\eta_l}^{\eta_u} \left[\frac{2}{\sqrt{3}}\varepsilon_{\eta\eta}\right] d\eta \tag{42}$$

$$= \frac{4}{\sqrt{3}}\sigma_0 Vt\, \upsilon_0 \tag{43}$$

where η_l and η_u denote lower and upper boundaries for the strain field in the lateral direction on one side of the center line and υ_0 is half of the maximum gap width between the plate curls in front of the wedge.

In Appendix A it is shown that

$$\upsilon_0 \approx 0.16 R\cos^2\theta(1 + 0.55\theta^2) \tag{44}$$

giving the final expression as

$$\dot{E}_c = \frac{0.64}{\sqrt{3}}\sigma_0 Vt R\cos^2\theta(1 + 0.55\theta^2). \tag{45}$$

7.2. Far field, membrane deformation

As discussed in Section 5, we assume that material over the PT–PQ gap shown in Fig. 6 is accommodated by shear strains; the plate deforms as a bundle of longitudinal inextensible chords.

From Eqn (35) the rate of energy dissipation is found as an integral of the equivalent strain over the width of the plastic zone in the wake of the wedge, for example along the PT-line (see Fig. 6):

$$\dot{E}_m = 2\sigma_0 V t \int_{\eta_P}^{\eta_T} \left[\frac{2}{\sqrt{3}}\varepsilon_{\xi\eta}\right] d\eta \tag{46}$$

$$2\sigma_0 V t \int_{\eta_P}^{\eta_T} \left[\frac{2}{\sqrt{3}}\frac{1}{2}\left(\frac{\partial u}{\partial \eta} + \frac{\partial v}{\partial \xi}\right)\right] d\eta \tag{47}$$

$$\frac{2}{\sqrt{3}}\sigma_0 V t[u_P - u_T] = \frac{2}{\sqrt{3}}\sigma_0 V t\, u_0 \tag{48}$$

where u_0 is the distance between Q and T in Fig. 6. In Appendix A it is shown that $u_0 \approx B\,\theta$ so the final

expression becomes

$$\dot{E}_{\mathrm{m}} = \frac{2}{\sqrt{3}}\sigma_0 V t B\theta. \tag{49}$$

7.3. *Far field, bending*

As illustrated in Fig. 6, the steady-state cutting process involves several areas of bending. The relevant bending radii are the radius at the side of the wedge, R, and the radius in front of the wedge, R_t. For point T to be at the shoulder wedge, the relation between these radii becomes:

$$R_t = R\cos\theta. \tag{50}$$

The three primary bending mechanisms are:

1. initial curling—the curvature of the undeformed plate changes from 0 to $1/R_t$ (hinge line OP);
2. hinge lines at wedge front—the plate is straightened out so that the curvature is reverted from $1/R_t$ back to 0 for a part of the plate (hinge line CD); and
3. bending around the wedge shoulder (line PT).

The hinge lines of point 2 and 3 above are in areas of high membrane straining so if the true interaction on the yield curve Eqn (28) was taken into account these hinges would give very limited resistance and they are therefore neglected in the following.

Since the jump in curvature is $[\kappa_{nn} = 1/R_t = 1/R\cos\theta$ and the total width of the hinge line perpendicular to the direction of motion is $B+R$, the final expression for the rate of energy dissipation due to bending becomes (see Eqn (37)):

$$\dot{E}_{\mathrm{b}} = 2\int V M_0[\kappa_{nn}]\mathrm{d}\eta \tag{51}$$

$$= \frac{\sigma_0 t^2(B+R)V}{\sqrt{3}R\cos\theta}. \tag{52}$$

8. FRICTION AND PERPENDICULAR REACTION

Friction is an important energy dissipating mechanism. Wierzbicki and Thomas [33] and Ohtsubo and Wang [18] use a factor for the effect of friction on the plate resistance:

$$g = \frac{F}{F_{P,c}} = 1 + \frac{\mu}{\tan\theta} \tag{53}$$

which indicates that friction increases the resistance by 52% for the example of μ=0.3 and θ=30°. In a study of tube splitting on a flat die, Stronge *et al.* [26] use a friction factor of g=1/(1−μ). For the case of aluminium against a steel die they measure a coefficient of friction of μ=0.56 giving a friction factor of g=2.27.

As indicated by Eqn (27) we assume a Coulomb type of friction where the frictional stress at the interface between plate and wedge is proportional to the normal pressure and it is shown below that the friction factor, g, can then be consistently derived from Eqn (27) and requirement of equilibrium. Noting that the surface S in Eqn (27) is plane and assuming that V_{rel} is constant over this surface gives the expression:

$$F \cdot V = F_{P,c} \cdot V + 2\mu N V_{\mathrm{rel}} \tag{54}$$

where N is the normal force on one of the front wedge sides.

The relative velocity, V_{rel} between the plate and the wedge at the contact area is assumed to be inclined an angle, ζ, from the plane of the plate (Fig. 8). This angle depends on the rolling of the plate curls on the wedge and it can be shown that ζ must be bound by 0 and θ, $0 \le \zeta \le \theta$.

Pippenger [21] reports scouring traces on a θ=45° wedge to have ζ=22.5° and ζ=17.9° for experiments with α=70° and α=45°, respectively. As an estimate we will thus use $\zeta=\theta/2$ which also makes sense intuitively.

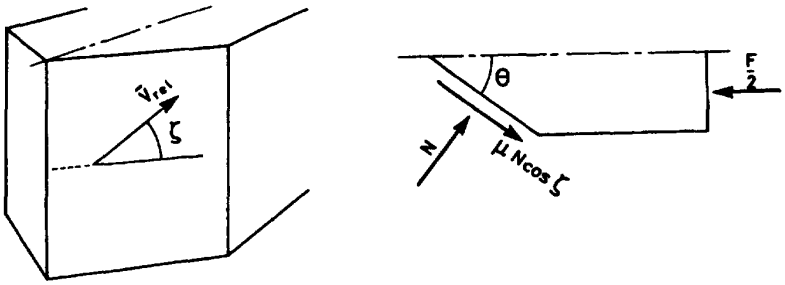

Fig. 8. Definition of direction of relative velocity and free body diagram for wedge.

The tangential friction force on the wedge is in the same direction as V_{rel}. Figure 8 shows the direction of V_{rel} and a free body diagram of the wedge.

It is seen that horizontal equilibrium can be expressed as

$$\frac{F}{2} = N\sin\theta + \mu N\cos\theta\cos\zeta \tag{55}$$

$$N = \frac{F}{2(\sin\theta + \mu\cos\theta\cos\zeta)}. \tag{56}$$

Inserting into Eqn (54) gives

$$F = F_{P,c}\left(1 - \frac{\mu}{\sin\theta + \mu\cos\theta\cos\zeta}\right)^{-1}. \tag{57}$$

If we use considering the example of $\theta=\pi/2$ and $\zeta=\pi/2$, corresponding to the tube splitting process, the friction factor becomes $g=1/(1-\mu)$ which is the same expression as used by Stronge *et al.* [26].

Inserting $\zeta=\theta/2$ in Eqn (56) gives the final expression for the friction factor:

$$g(\mu,\theta) = \frac{F}{F_{P,c}} = \left(1 - \frac{\mu}{\sin\theta + \mu\cos\theta\cos(\theta/2)}\right)^{-1}. \tag{58}$$

It is seen that this expression is different from that used by Wierzbicki and Thomas [33], and Ohtsubo and Wang [18] Eqn (53). Equation (53) gives lower values for g than our Eqn (58). At $\mu=0.3$ and $\theta=10°,30°, 45°$ the difference is 3.2%, 9.0% and 13%, respectively.

The reaction force, F_V on the *plate* perpendicular to the direction of motion is the vertical component of the friction force μN:

$$F_V = -2\mu N\sin\zeta = F\frac{-2\mu\sin\zeta}{2(\sin\theta + \mu\cos\theta\cos\zeta)}. \tag{59}$$

With $\zeta=\theta/2$ the ratio between the vertical reaction and the horizontal resistance thus becomes

$$k(\mu,\theta) = \frac{F_V}{F} = \frac{-\mu\sin(\theta/2)}{\sin\theta + \cos\theta\cos(\theta/2)}. \tag{60}$$

Using the approach described above, Pippenger [21] has derived the relations corresponding to Eqns (58) and (60) for the case of a wedge which is inclined an angle, α (see Fig. 2), from the direction perpendicular to the plate. Keeping the relations in their most general form but modifying Pippenger's expressions according to the assumption $V_{rel}=V$, we get:

$$\frac{F}{F_{P,c}} = g(\mu,\theta,\alpha) = \left(1 - \frac{\mu}{\sin\beta\sin\theta' + \mu(\cos\theta'\cos\zeta + \sin\zeta\cos\beta\sin\theta')}\right)^{-1}. \tag{61}$$

$$\frac{F_V}{F} = k(\mu,\theta,\alpha) = \frac{\cos\beta - \mu\sin\zeta\sin\beta}{\sin\beta\sin\theta' + \mu(\cos\theta\cos\zeta + \sin\zeta\sin\theta\cos\beta)} \tag{62}$$

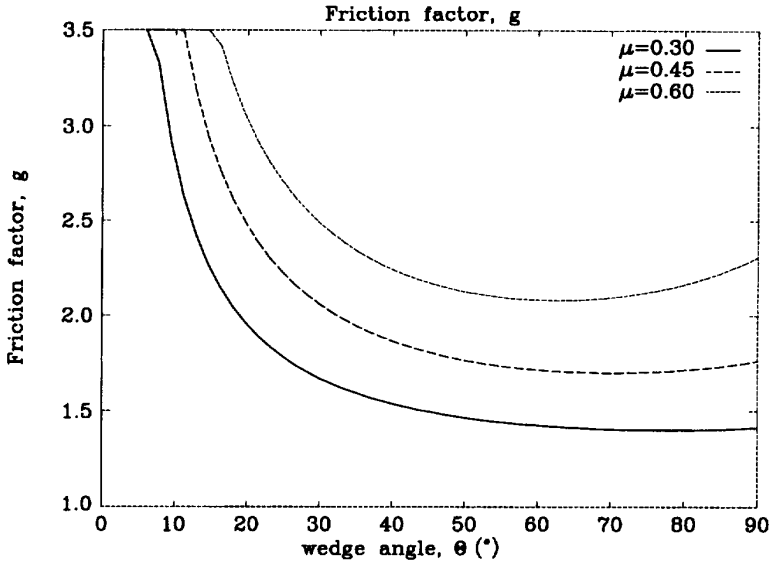

Fig. 9. Friction factor, g (μ=0.3, 0.45, 0.6 and α=10°).

where θ' is the projected wedge angle and β is an intermediate value:

$$\theta'(\theta, \alpha) = \tan^{-1}(\tan\theta \cos\alpha) \tag{63}$$

$$\beta(\theta, \alpha) = \tan^{-1}(1/\tan\theta' \tan\alpha). \tag{64}$$

For α=0, it is seen that $\theta' = \theta$, β=π/2 and with ζ=θ/2 Eqns (61) and (62) reduce to Eqns (58 and 60) as expected.

Fig. 9 shows the friction factor, g, as a function of wedge angle, θ, for μ=0.3, 0.45, 0.6 and α=10°. Taking μ=0.3, α=10°, and θ=10°, 30° and 45° gives friction factors, g, of 2.8, 1.7 and 1.5, respectively indicating a very significant contribution of friction to the total plate resistance.

It should be noted that the effect of friction comes as a factor which is independent of the rolling radius, R. Likewise, the plastic/fracture resistance derived in the previous section was found to be independent of μ so the radius which minimizes the resistance force becomes independent of μ. This does not probably reflect reality for the tube splitting process, Stronge *et al.* [26] use an expression for the plate rolling radius which is a strong function of μ but at present there is not sufficient information available about this problem to improve the model in this respect.

Also, it should be noted that all of the contact pressure is assumed to be on the front plane sides of the wedge. However, the cornerpoint at the shoulders and the front tip might transmit some force. The effect of the shoulders will tend to increase the friction factor whereas the force on the front tip tends to lower it. For wedges with sharp edges the effect of these edge irregularities is believed to be small but for some types of idealized rocks, like for example the cone shaped rock analyzed by Rodd and MacCampbell [22], these effects are dominating and prediction of g and k becomes a cumbersome task.

Fig. 10 shows k as a function of wedge inclination angle, α, for θ=45° and μ=0.3, 0.45, 0.6. For small inclination angles, α, the vertical component of the frictional force dominates over the normal force, and the total vertical force is thus negative.

9. TOTAL REACTION AND VERIFICATION

The problem of two alternative deformation modes in the tip zone in front of the cutting edge was described in Sections 5 and 6. The resistance force is derived for both alternative modes below.

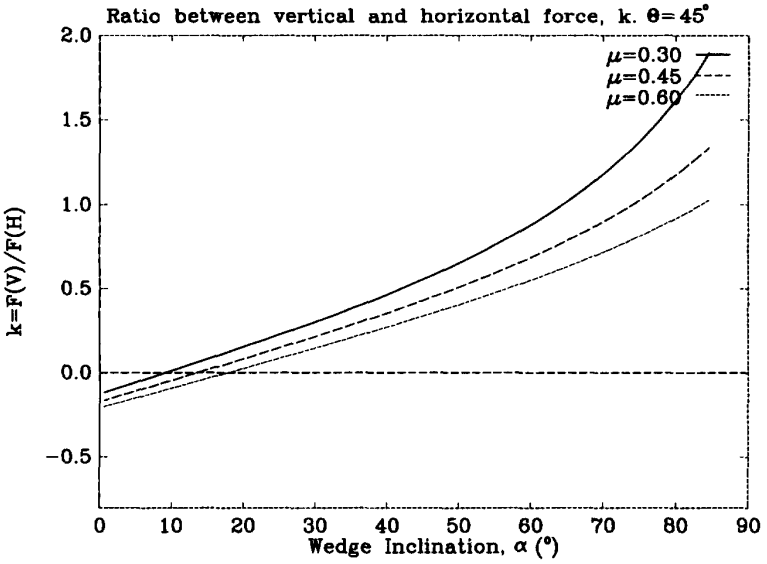

Fig. 10. Ratio between vertical and horizontal force, k (θ=45° and μ=0.3, 0.45, 0.6).

Combining Eqns (27, 45, 49, 52 and 61) gives the plastic/fracture resistance force on the plate for the mode where the crack does not run ahead of the wedge:

$$F = g(\mu,\theta,\alpha)\frac{\dot{E}_c + \dot{E}_m + \dot{E}_b}{V}$$

$$= g(\mu,\theta,\alpha)\left\{\frac{0.64}{\sqrt{3}}\sigma_0 t R\cos^2\theta(1+0.55\theta^2) + \frac{2}{\sqrt{3}}\sigma_0 t B\theta + \frac{\sigma_0 t^2(B+R)}{\sqrt{3}R\cos\theta}\right\} \tag{65}$$

$$R \le B\frac{1}{\pi/2-1} = 1.75B. \tag{66}$$

The limit of R (Eqn (66)) comes from the general kinematic requirement that the deformed plate flaps must be in contact with the wedge. The rolling radius, R, which gives the lowest resisting force becomes

$$R = \sqrt{\frac{Bt}{0.64(1+0.55\theta^2)\cos^3\theta}}. \tag{67}$$

In the alternative crack-tip deformation mode where the crack runs ahead of the wedge, the rate of energy dissipation in the tip zone is not a function of R and the total rate of energy dissipation therefore does not have a mathematical minimum as above; it is a monotonically decreasing function of the rolling radius. Using the maximum allowable rolling radius for kinematic consistency, Eqns (27, 39, 49 52 and 61) then gives the resistance force as

$$F = g(\mu,\theta,\alpha)\left\{G_c t + \frac{2}{\sqrt{3}}\sigma_0 t B\theta + \frac{1.57\sigma_0 t^2}{\sqrt{3}\cos\theta}\right\}. \tag{68}$$

In order to verify the derived equations, the experimental results showed in Section 2 are considered again. Application of Eqn (68) imposes the difficulty that the fracture parameter, G_c is unknown. Lu *et al.* [15] performed an experimental study on tearing energy in splitting metal tubes and presented an expression and test results for mild steel plates which seems to be independent of plate thickness (at least for thicknesses between 0.5 and 1.5 mm):

$$G_c = 8.8\,\text{mm}\sigma_u\varepsilon_f. \tag{69}$$

Table 5. Steady state cutting: theoretical predictions and experimental results for three tests

Experiments by	g from Eqn (58)	R (mm) Eqn (67)	F (kN) Eqn (65)	F (kN) Eqn (68)	F (kN) Measured
1. Lu and Calladine [13]	2.81	3.59	5.58	5.72	6.0
2. Yahiaoui *et al.* [35]	1.50	4.85	3.53	3.58	2.5
3. Astrup [5]	1.67	72.3	2372	1722	2250

Table 6. Partitioning of energy between deformation mechanisms and friction. Calculation model assumes a purely plastic flow at wedge tip, $E_{tot}=E_c+E_b+E_m$

Experiments by	Friction $\frac{g-1}{g}$	Front tip $\frac{E_c}{E_{tot}}$	Shear $\frac{E_m}{E_{tot}}$	Bending $\frac{E_b}{E_{tot}}$	$\frac{E_m+E_b}{E_c}$
1. Lu and Calladine [13]	64%	29%	22%	49%	2.5%
2. Yahiaoui *et al.* [35]	33%	10%	74%	16%	8.7%
3. Astrup [5]	40%	17%	56%	27%	4.9%

Assuming that the separation process in plate cutting resembles that of tube splitting, this relation is applied below. However, as also stated by Lu *et al.* [15], the parameter G_c is a crude one to use in other problems than the specific one considered in the test, because the tearing energy is highly dependent the detailed stress–strain state in the process. This was also noted by Atkins [7], who reported values for G_c ranging from 200–1000 kJ/m^2 depending on the type of tearing process. Therefore, to apply expressions like Eqns (68) and (69) really requires further work on the detailed ductile separation process.

The friction factors, g, in the following verification examples are calculated from Eqn (61) using $\mu=0.3$ and $\alpha=10^\circ$. The fracture strains of the three experiments are assumed to be 0.25, 0.25 and 0.15, respectively giving fracture toughnesses of 600, 600 and 700 kJ/m^2.

Table 5 shows a comparison between the theoretical prediction of the two presented models and the experimental results which were also presented in Table 3.

The theory, Eqn (65) with Eqn (67), over-predicts the forces of the three reported tests by −7%, 41% and 5%. Thus, except for the test of Yahiaoui [35], there is seen to be very good agreement between theory and experiments even though the scale of the problems is different by an order of magnitude. Also, it is noted that the difference between the two calculation models, Eqns (65) and (68) is small. If values for the fracture toughness G_c were sufficiently accurate the relative magnitude of the numbers in column four and five would indicate which of the two presented models would develop. The actual numbers in Table 5 indicate that the plate was cut (purely plastic flow) in the two experiments with thin plates but it fractured in the experiment of Astrup [5]. Actually, this seems to be in accord with the reported experimental results.

Table 6 shows how the energy dissipation is distributed between deformation mechanisms and friction when the plate resistance is calculated from Eqn (65).

It is interesting to note how differently the energy is distributed in the three examples due to different wedge angles, plate thicknesses and wedge width, and it indicates why it is difficult to derive formulas that capture all dependencies on a purely empirical basis. Also, it is noted that the effect of friction is significant. The last column in Table 6 shows the importance of the far field deformation relative to the tip zone process. It is clear that the far field energy dissipation is dominant in these examples. The corresponding values for the alternative model with material fracture instead of plastic flow at the crack tip are $\chi=1.12$, 4.31 and 72.5. These values of χ are the ones to be used if we were to scale the results according to the scaling formula presented by Atkins Eqn (15), assuming a fracture process at the crack tip.

10. CONCLUSIONS

The paper presents a literature review and develops new formulas for calculating the resistance of a ductile plate being cut by a wedge of finite width.

Most of the published results on plate cutting is concerned with initiation cutting rather than the steady-state cutting which develops if the wedge has a finite width. Analysis of previously published work shows a significant difference between proposed formulas and attempts to use the proposed formulas for predicting published experimental results did not show a convincing overall agreement.

The presently proposed theoretical model is based on the energy dissipation rate in an assumed deformation mode consisting of a plastic-tip zone, moving bending hinge lines and a membrane deformation zone. It is shown how the analysis simplifies if the membrane deformation zone is assumed to be dominated by plastic shear strains. Attempts were made to model the tip zone both by a purely plastic flow mode and by a plastic fracture mode governed by the material fracture toughness. However, it is recognized that more work is needed to fully understand contribution of the tip zone in cutting and tearing deformation mode. Dynamic effects are not included, so far, for application to real scale groundings the presented analysis model should be extended to cover at least strain rate effects. Friction was taken into account and formulas were derived both for the so called friction factor and for the vertical to horizontal force ratio.

A comparison of the proposed formulas with experiments of Lu and Calladine [13], Astrup [5], and Yahiaoui *et al.* [35] shows a good overall agreement.

Acknowledgements—All drawings were carefully prepared by Hugo Heinicke. The work is greatly acknowledged.

APPENDIX A. MODEL GEOMETRY

The objective of this section is to find the gap openings u_0 and $2v_0$, shown in Fig. 6, expressed in terms of the rolling radius $R(=R_t/\cos\theta)$, the wedge shoulder width, $2B$ and the wedge semi angle, θ.

A.1. Gap opening at wedge front

It is convenient to introduce two coordinate systems, a global system, $(X,Y,Z)_G$ and a local system,$(x,y,z)_l$, both with origin at point O. The z-and Z-axes point vertically upwards, the X_G-axis is in the symmetri line pointing towards the wedge tip and the x_l-axis is in the bending hinge line, OP. The y_l–Y_G-axes are defined from the other axes. An arc line coordinate, s, which follows the curling edge of the plate is also introduced (see Fig. 11). The s-axis also has the origin at point O.

A point on the edge with the arc line coordinate, s, has the local coordinates

$$x_l = s\cos\theta$$
$$y_l = -R_t \sin\left(\frac{s\sin\theta}{R_t}\right) \tag{A.1}$$
$$z_l = R_t\left(1-\cos\left(\frac{s\sin\theta}{R_t}\right)\right).$$

The general relation between local and global coordinates is given by the transformation:

$$X_G = x_l\cos\theta - y_t\sin\theta$$
$$Y_G = x_l\sin\theta + y_l\cos\theta \tag{A.2}$$
$$Z_G = z_l.$$

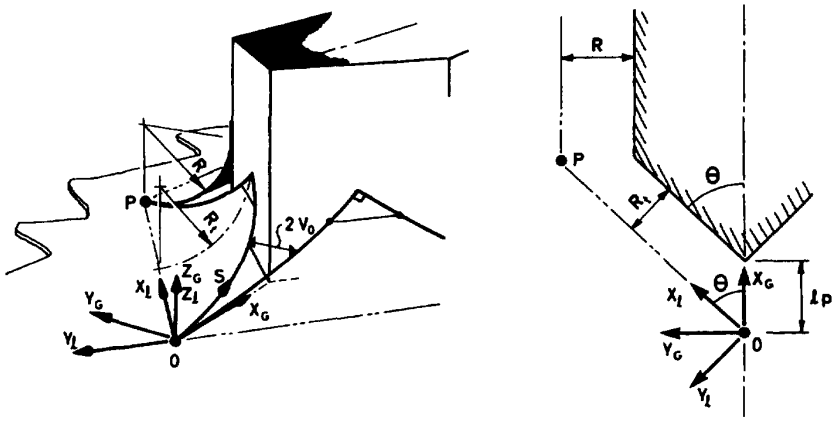

Fig. 11. Definitions used for finding the gap width at the wedge tip.

Inserting Eqns (A.1 and A.2) gives the global coordinates for a point on the plate edge with coordinate s:

$$X_G = (s\cos\theta)\cos\theta - \left(-R_t \sin\left(s\sin\frac{\theta}{R_t}\right)\right)\sin\theta \tag{A.3}$$

$$Y_G = (s\cos\theta)\sin\theta + \left(-R_t \sin\left(\frac{s\sin\theta}{R_t}\right)\right)\cos\theta \tag{A.4}$$

$$Z_G = z_1. \tag{A.5}$$

Since the gap opening is $2v_0 = 2Y_G$ it is now given from Eqn (A.4) as a function of s, R and θ:

$$2v_0 = 2\left(s\cos\theta\sin\theta - R\cos^2\theta\sin\left(\frac{s}{R}\tan\theta\right)\right) \tag{A.6}$$

The objective is to find the gap width at the cutting edge, i.e. at the point where $X_G = l_p = R_t/\sin\theta = R/\tan\theta$ (see Fig. 11). Eqn (A.3) is too complex to be solved in a closed from for s, otherwise this value of s should be inserted into Eqn (A.6) giving a the final expression sought. It has to be done numerically.

As an initial guess we could calculate the gap width at $s = l_p = R/\tan\theta$. From Eqn (A.6) the expression becomes:

$$2v_0 = 2R\cos^2\theta(1 - \sin 1) = 0.317R\cos^2\theta. \tag{A.7}$$

By comparing this expression to the exact solution found from numerical solution of Eqns (A.3) and (A.6) it is found that the expression for the gap width, $2v_0$ at the cutting edge is very well approximated by the expression:

$$2v_0 = 0.317R\cos^2\theta(1 + 0.55\theta^2). \tag{A.8}$$

The error of Eqn (A.8) at 10°, 30°, 45° is, respectively, 0.25%, 1.3% and 0.18%.

A.2. Gas opening at wedge shoulders

It is convenient to define a coordinate, (X,Y,Z), at the shoulder in the plane of the undeformed plate. The Z-axis points vertically upwards along the shoulderline, the Y-axis is in the plane of the undeformed plate and it is perpendicular to the Z-axis and to the wedge sides. The X-axis is defined from the Y-and Z axes (see Fig. 12)

The total width of the deformed plate on one side of the symmetry line is $R+B$ and the length of the curved part of the flap is $\pi R/2$ so the width of the straight part of the flap at the wedge sides becomes

$$b_{fs} = (R + B) - \pi R/2 = B - R(\pi/2 - 1) \tag{A.9}$$

Likewise, it can be shown that the width of the straight part of the flap at the wedge front becomes

$$b_{ff} = \cos\theta(B - R(\pi/2 - 1)). \tag{A.10}$$

We require the tangent of the deformed plate flaps to conform to the wedge as shown in Fig. 12 giving the requirement

$$b_f \geq 0 \tag{A.11}$$

$$R \leq \frac{B}{\pi/2 - 1} \approx 1.75B. \tag{A.12}$$

The position of point T is

$$\begin{pmatrix} X \\ Y \\ Z \end{pmatrix}_T = \begin{pmatrix} 0 \\ 0 \\ B + R(2 - \pi/2) \end{pmatrix}, \tag{A.13}$$

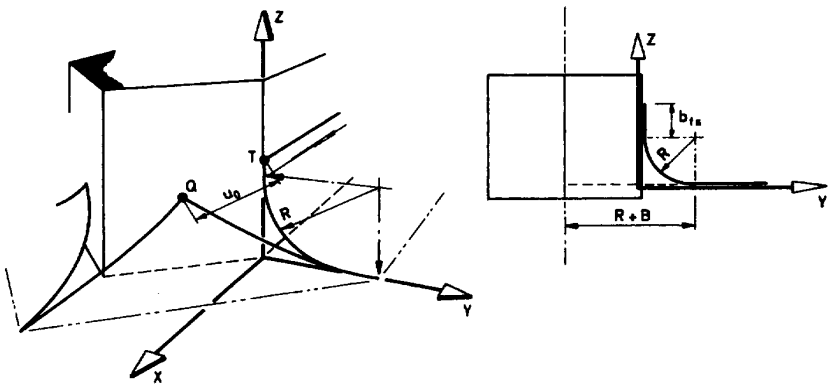

Fig. 12. Definitions used for finding the gap width at the wedge sides.

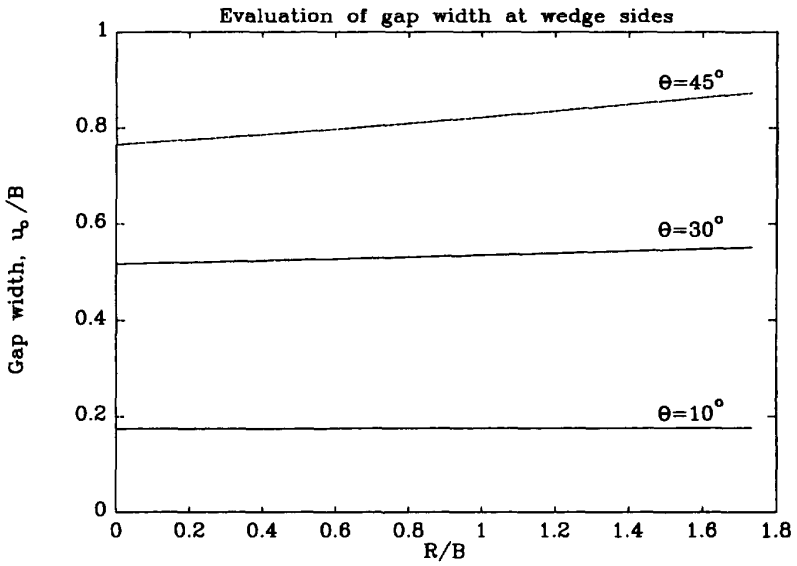

Fig. 13. Variation of the gap width with rolling radius.

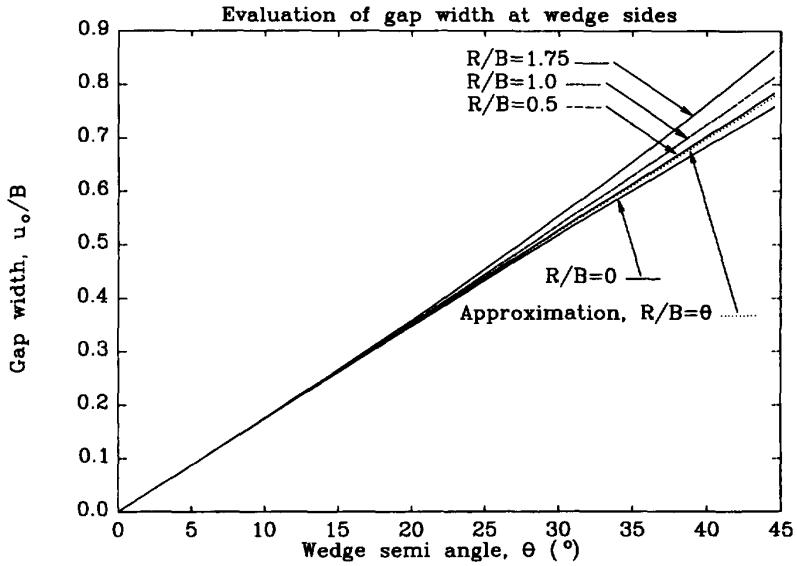

Fig. 14. Variation of the gap width with wedge angle.

and the position of point Q is:

$$\begin{pmatrix} X \\ Y \\ Z \end{pmatrix}_Q = \begin{pmatrix} B\sin\theta\cos\theta \\ -B\sin^2\theta \\ (B + R(2 - \pi/2))\cos\theta \end{pmatrix} \tag{A.14}$$

The distance between T and Q is then given by:

$$\begin{aligned} u_0 &= ((X_T - X_Q)^2 + (Y_T - Y_Q)^2 + (Z_T - Z_Q)^2)^{0.5} \\ &= (B^2\sin^2\theta + (1 - \cos\theta)^2(B + R(2 - \pi/2))^2)^{0.5} \end{aligned} \tag{A.15}$$

Figs 13 and 14 show the variation of the gap width with rolling radius and wedge angle from Eqn (A.15).

It is seen from Fig. 13 that u_0/B is a very weak function of the rolling radius and Fig. 14 illustrates that Eqn (A.15) is well approximated by the expression

$$u_0 = B\theta \tag{A.16}$$

for the considered ranges of θ and R.

REFERENCES

1. Abramowicz, W. and Wierzbicki T., Axial crushing of foam filled columns, *Int. J. of Mech. Sci.*, 1988, **30**(3/4), 263–271.
2. Akita, Y., Ando, N., Fujita, Y. and Kitamura K., Studies on collision-protective structures in nuclear-powered ships, *Nucl. Engng Design*, 1972, **19**, 365.
3. Akita, Y. and Kitamura, K., A study on collision by an elastic stem to a side structure of ships, *J. Soc. of Naval Architects of Japan*, 1972, **131**, 307–317.
4. Alexander, J.M., An approximate analysis of the collapse of thin cylindrical shells under axial loading, *Quarterly J. Mech. and Appl. Math.*, 1969, **13**, 10–15.
5. Astrup, O., Cutting of thick plates by a wedge, Joint MIT-Industry Project on Tanker Safety, 27 Jan 1994.
6. Atkins, A.G., Scaling in combined plastic flow and fracture, *Int. J. Mech. Sci.*, 1988, **30**, 173.
7. Atkins, A.G., Tearing of thin metal sheets, *Structural Failure* eds T. Wierzbicki and N. Jones, John Wiley and Sons, 1989, 107–132.
8. Atkins, A.G., Letter to the editor, *Int. J. Mech. Sci.*, 1991, **33**, 69–71.
9. Jones, N., Scaling of inelastic structures loaded dynamically, *Structural Impact and Crashworthiness*, Vol 1, ed. G.A.O. Davies, Elsevier Science, Amsterdam, 1984, 45–74.
10. Jones, N., Quasi-static analysis of structural impact damage, *J. Construct. Steel Research*, 1995, **33**, 151–177.
11. Jones, N. and Jouri W.S., A study of plate tearing for ship collision and grounding damage, *J. Ship Research.*, 1987, **31**, 253.
12. Jones, N., Jouri, W.S. and Birch, R.S., On the scaling of ship collision damage, *3rd International Congress on Marine Technology*, Athens, Greece, International Maritime Association of East Mediterranean, Phivos, 1984, 287–294.
13. Lu, G. and Calladine, C.R., On the cutting of a plate by a wedge, *Int. J. Mech. Sci.*, 1990, **32**, 295–313.
14. Lu, G. and Calladine, C.R., Author's reply, *Int. J. Mech. Sci.*, 1984, **33**(1), 73–74.
15. Lu G., Ong, L.S., Wang, B. and Ng, H.W., An experimental study on tearing energy in splitting square metal tube, *Int. J. Mech. Sci.*, 1994, **36**, 1087–1097.
16. Maxwell, L.M., *Effect of rock geometry on the failure modes of plates and the forces in grounding experiments*, Technical Report 15, Joint MIT-Industry Program on Tanker Safety, May (1993).
17. Minorsky, V.U., An analysis of ship collisions with reference to protection of nuclear power plants, *J. Ship Research.*, 1959, **3**, 1–4.
18. H. Ohtsubo, G. Wang, An upper-bound solution to the problem of plate tearing, *J. Marine Sci. Technol.*, **1**, 1995.
19. Paik, J.K., Cutting of a longitudinally stiffened plate by a wedge, *J. Ship Research*, 1994, **38**(4), 340–348.
20. Paik, J.K., Lee, T.K., Cutting tests for a stiffened plate by a wedge, *MARIENV*, Tokyo, September, 1995.
21. Pippenger, D., *Coupled vertical and horizontal resistance of hull girder in grounding accidents*, Technical Report 46, Joint MIT-Industry Program on Tanker Safety, May, 1995.
22. Rodd, J.L. and MacCampbell, S., Double hull tanker grounding experiments, *The Advanced (unidirectional) Double-Hull Technical Symposium*, Gaithersburg, Maryland, 1994.
23. Simonsen, B.C. and Wierzbicki, T., Grounding bottom damage and ship motion over a rock, *Int. J. Offshore Polar Engng*, 1996, **6**(3), 195–202.
24. Simonsen, B.C., Wierzbicki, T. and Choi, S.K., *Theoretical manual on grounding damage of a hull bottom structure*, Vol. i, Technical Report 52, Joint MIT-Industry Program on Tanker Safety, June, 1995.
25. Stronge, W.J., Yu, T.X. and Johnson, W., *Energy dissipation by splitting and curling tubes*, Vol. 2, ed. J. Morton, Applied Science, London, 1983, pp. 576–587.
26. Stronge, W.J., Yu, T.X. and Johnson, W., Long stroke energy dissipation in splitting tubes, *Int. J. Mech. Sci.*, 1984, **25**, 637–647.
27. Thomas, P.F., *Application of plate cutting mechanics to damage prediction in ship grounding*, Joint MIT-Industry Project on Tanker Safety, 8, May 1992.
28. Turgeon, J., *Analysis of hull damage without fracture in single-bottom transversally framed ships subjected to grounding*, Technical Report 48, Joint MIT-Industry Program on Tanker Safety, May, 1995.
29. Vaughan, H., Bending and tearing of plate with application to ship bottom damage, *The Naval Architect*, 1978, **3**, 97–99.
30. Vaughan, H., The tearing of mild steel plate, *J. Ship Research*, 1980, **24**(96), 96.
31. Wierzbicki, T., *Concertina tearing of metal plates—improved solution and comparison*, Joint MIT-Industry Project on Tanker Safety, 22, 1994.
32. Wierzbicki, T. and Abramowicz W., On the crushing mechanics of thin-walled structures, *J. Appl. Mech.*, 1983, **5**, 727–734.
33. Wierzbicki, T. and Thomas, P., Closed-form solution for wedge cutting force through thin metal sheets, *Int. J. Mech. Sci.*, **35**, 1993.
34. Woisin, G., Comments on Vaughan: the tearing strength of mild steel plate, *J. Ship Research*, 1987, **26**(1), 50–52.
35. Yahiaoui, M., Bracco, M., Little, P. and Trauth, K., *Experimental studies on scale models for grounding*, Technical Report 18, Joint MIT-Industry Program on Tanker Safety, Jan, 1994.
36. Zheng, Z.M. and Wierzbicki, T., *Steady-state wedge indentation—improved theory and validation*, Joint MIT-Industry Project on Tanker Safety, 42 (1995).